PAPER • OPEN ACCESS

Fragility Curves for Assessing the Seismic Vulnerability of Multi-Drum Ancient Columns

View the article online for updates and enhancements.

Fragility Curves for Assessing the Seismic Vulnerability of Multi-Drum Ancient Columns

Fabio Di Trapani[1], Vasilis Sarhosis[2], Giovanni Tomaselli[1], Gabriele Bertagnoli[1]

[1]Dipartimento di Ingegneria Strutturale, Edile e Geotecnica, Politecnico di Torino (PoliTo), Corso duca degli Abruzzi, 24, 10129 Turin, Italy
[2]School of Civil Engineering, University of Leeds, Woodhouse Ln, Woodhouse, Leeds LS2 9DY, UK

gabriele.bertagnoli@polito.it

Abstract. The paper deals with an assessment of the seismic fragility of multi-drum ancient columns in the probabilistic assessment framework of incremental dynamic analysis (IDA). The dynamic response of multi-drum ancient is governed by the motion of stone-drums which can rock and slide individually or in group, individuating different possible collapse mechanisms, which are also depending on ground motion intensity. In this research, two different in geometry columns i.e. different height and number of drums analysed. The columns were modelled using the UDEC software based on the discrete element method (DEM). IDA was carried out for 10 ground motion records with and without considering the vertical component of earthquake excitation, in order to assess also its influence on the resulting fragility. Results are provided in terms of fragility curves and allow evaluating the influence of the geometrical assembly of the columns and vertical component of the ground motions.

1. Introduction

Natural events such as earthquakes represent a major threat to cultural heritage structures including ancient temples [1, 2]. Ancient temples consist of multi-drum or monolithic columns made of marble or limestone. Multi-drum columns were constructed by placing each drum (or block of stone) on top of each other. Thus, during shaking of the ground, drums are free to rock and slide, either individually or in groups. Today, due to damage, destruction, and restoration purposes, many of the ancient columns are free standing, which makes them more vulnerable to the earthquake load [3]. Over the last decades, the dynamic performance of ancient freestanding columns has received increasing scientific attention. Mainly, this was to understand their seismic performance and better select conservation and rehabilitation techniques for their survival during strong earthquakes. In the last four decades, many researchers studied the rocking response of rigid blocks analytically, numerically, and experimentally [4-6]. In addition, over the last three decades, advanced computational methods were used to solve numerical procedures to evaluate the response performance of multi-drum columns subjected to strong seismic excitations. An alternative to the available FEM is the Discrete (or distinct) Element Method (DEM). DEM was developed by Cundall for evaluating the stability of jointed or fractured rocks [7, 8]. The key features of the method are: a) blocks can be represented as rigid or deformable; b) large displacement and rotation of blocks are allowed; c) new contacts are automatically detected as the simulation proceeds [8, 9]. The two-dimensional (2D) discrete element software UDEC was used by

Psycharis et al. [10] to investigate the in-plane seismic response of two multi-drum columns and identify their stability under earthquake excitations. They found that earthquakes with large dominant periods are more threatening than short-period ones for multi-drum columns. In addition, the seismic reliability of multi-drum columns has been studied by Psycharis et al. [11] with the use of synthetic ground motions obtained from a stochastic analysis using Monte-Carlo simulations. The aim of this paper is to investigate the dynamic response of ancient multi-drum columns subjected to horizontal and combined horizontal and vertical harmonic excitations. Using a software based on the Discrete Element Method (DEM), two typical ancient multi-drum columns were subjected to incremental dynamics analysis (IDA) to derive their fragility curves. With respect to existing contributions dedicated to the harmonic response of monolithic and multi-drum columns, this work considers the combined effect of horizontal and vertical seismic components on column collapse and maximum displacements, showing that collapse conditions and displacements increase significantly with respect to the simpler case of horizontal excitation.

2. Reference case studies

The archaeological literature presents a huge variety of columns characterized by different geometrical dimensions and variable number and shape of blocks, [12,13] are shown in figures 1 and 2.

The assessment of seismic vulnerability of columns depends on the reproduction of the real imperfections of the column and on the strong sensitivity of the structure to small changes of the geometric and seismic features. The geometric features undergo imperfection caused by past earthquakes. The most common imperfections are [13]:

-       collapsed parts of the structure, which reduce the contact areas;
-       foundation problems, which can cause the tilting of the columns;
-       residual displacements of the drums, due to previous earthquakes;
-       cracking of the structural elements, which can sometimes split the blocks into two parts.

Past research has demonstrated that the seismic response is governed by the main vibration period [14]. Low frequencies can cause an intensive rocking of the column, while high one may cause a sliding motion between the blocks which increases proportionally to the quote of the drum [15, 16]. For this reason, the choice of the ground motions to be used in the non-linear dynamic analysis must be accurate. In order to provide a framework for future studies, it was decided to analyse two simplified limit cases, namely a low column composed by 4 drums (case *a*) and a high column composed by 14 drums (case *b*). The two case studies are shown in figure 1. The properties of the columns are summarized in table 1. As it can be observed the overall slenderness ratio of the two columns (H/D_b) is similar, while the slenderness of the respective blocks (H_b/D_b) is quite different (Case *a* column blocks are three times more slender).
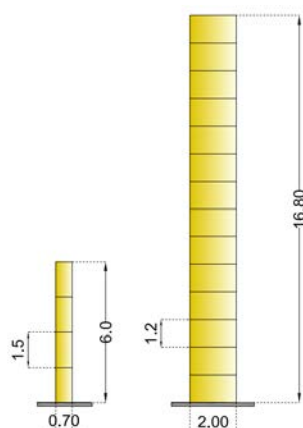

Figure 1. Geometric properties of the two case studies

Table 1. Geometric properties of the two selected columns

	H [m]	D_b [m]	n_d [-]	H_b [m]	H_b/D_b [-]	H/D_b [-]
Case a)	6.10	0.70	4	1.5	2.14	8.57
Case b)	16.80	2.00	14	1.2	0.60	8.40

3. Performance based earthquake engineering assessment framework

A performance-based earthquake engineering framework can be generally divided into four main steps: hazard analysis, structural analysis, damage analysis, and loss analysis (Cornell and Krawinkler, 2000 [17]). These steps are totally generic in the PBEE concept and hence they are here specialized to properly face specific issues which are typical of the structural systems under investigation. For the purpose of this framework, the first two steps are described in detail and used in the following sections.

3.1. Incremental Dynamic Analysis (IDA)

Incremental dynamic analyses (IDA) is adopted as a reference method to get a structural response. IDA has been recently widely employed by different authors (e.g. [18-24]) as it allows considering the uncertainty related to ground motions variability by obtaining a statistical distribution of the intensity measures inducing a limit state. In the current IDA framework, a set of 10 ground motions is scaled in amplitude up to the achievement of the specified limit states defined as limit engineering demand parameters (EDPs) or achievement of structural performances during the analyses (damage or collapse mechanisms). The ground motions set is first selected based on a spectrum compatibility criterion with respect to the site target spectrum. Selected ground motions are then scaled with respect to the peak ground acceleration (PGA), which is used IM. The obtained spectra, and the associated records, are then scaled up and down. Time history analyses are run for each ground motion at every scaling factor. IDA curves will provide the relationship between $IM = PGA$ and engineering demand parameters *(EDPs)* assumed at the achievement of structural performance.

3.2. Fragility analysis (derivation of fragility curves)

Results of IDA allow deriving fragility curves expressing the probability of exceeding a specified limit state as a function of a specified IM. Fragility curves can be represented using a lognormal cumulative distribution function (e.g. Baker 2015 [25]) using the following analytical expression:

$$P[\,C \leq D \,/\, IM = x\,] = \Phi\left(\frac{ln(\,x\,) - \mu_{ln(\,x\,)}}{\sigma_{ln(\,x\,)}} \right) \qquad (1)$$

where $P[\,C \leq D \,/\, IM = x\,]$ is the probability that a ground motion with $IM = x$ will cause the achievement of a limit state, Φ is the standard cumulative distribution function, $ln(\,x\,)$ is the natural logarithm of the variable x representing the intensity measure (PGA), $\mu_{ln(\,x\,)}$ and $\sigma_{ln(\,x\,)}$ are the mean and the standard deviation of the natural logarithms of the distribution of x, respectively. Fragility curves are derived for each monitored limit states during IDA. The definition of limit states for the investigated structures will be described in the following sections.

4. Structural modelling and limit states definition

4.1. Discrete Element Method (DEM) modelling of the columns

The discrete modelling approach was proposed for the first time in 1971 [7] to find a solution for problems due to rock mechanics, where distinct elements were used to simulate the movement of masses of rocks; thereafter this approach was extended to simulate the in-plane and out-of-plane behaviour of blocky masonry structures [13-16]. Within DEM, blocks can be assumed as rigid or

deformable elements. In this study, drums were assumed infinitely rigid. The latter assumption leads to many advantages from the computational point of view because accelerations are applied to each block centre of gravity. Blocks are connected to each other by a set of kinematical contact points which are placed on the external perimeter of the units, which use the contact hypothesis [8]. In this case, the contact interface is face-to-face, therefore consisting of a contact zone and two sub-contact zones (figure 2a); each contact zone has two different connections, one normal and one tangential, made by springs and dashboards. A sample of modelling (Case *b*) is illustrated in figure 2b.
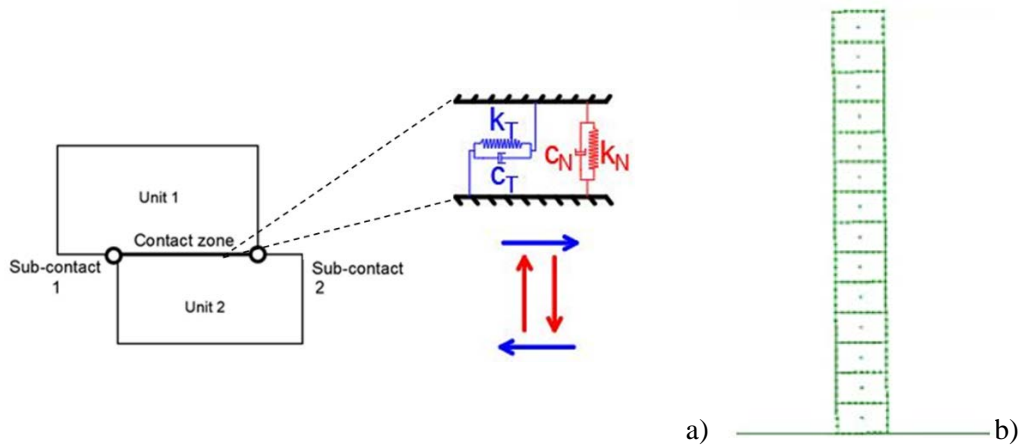

Figure 2. DEM modelling: a) Contact zones between two units; b) Case *b* model.

In the normal direction, the mechanical behaviour of the joints (i.e. the zero-thickness contact interface) is governed by the following equation:

$$\Delta\sigma_n = k_n \Delta u_n \qquad (2)$$

where is the normal stiffness of the contact and is the increment in normal contact displacement, i.e., the relative displacement between the blocks at the contact point. Similarly, in the shear direction, the mechanical behaviour is controlled by the constant shear stiffness using the following expression:

$$\Delta\tau_s = k_s \Delta u_s \qquad (3)$$

where is the change in shear stress, and is the increment in shear displacement.

4.2. Definition of ground motion set and scaling
Ten horizontal ground motions have been selected and scaled with respect to PGA to five intensity levels, namely 0.1,0.5,0.9,1.0 and 2.0 g. A sample of horizontal components ground motion spectra scaled to PGA=1 g is represented in figure 3. Two analysis scenarios have been considered: in the first, the sole horizontal component is used, while in the second, the respective vertical components are added in the analysis.
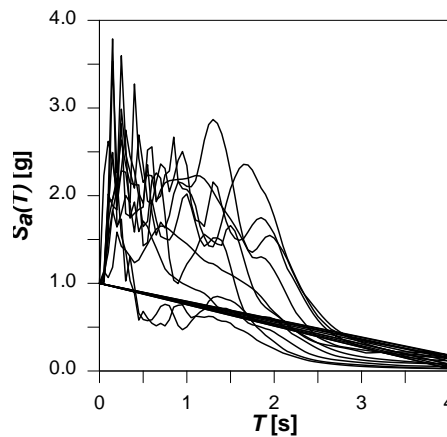
Figure 3. Ground motion spectra scaled with respect to 1.0 g PGA.

4.3. Definition of structural limit states

The maximum normalized displacement at the top (u_t) with respect to the base diameter (D_b) of the column is used as EDP [11] as shown in Eq. (4) and figure 4. Limit EDP values are assumed as suggested in [18] and illustrated in table 2.
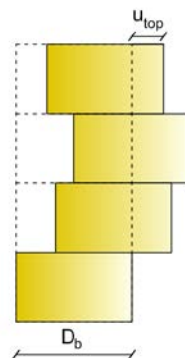
$$u_t = max\left(\frac{u_{top}}{D_b}\right) \tag{4}$$

Figure 4. Definition of the Engineering Demand Parameter (EDP) u_t.

Table 1. Limit EDP values of u_t [11]

u_t	Performance level	Description
0.15	Damage limitation	No danger for the columns. No permanent drum dislocations expected.
0.35	Significant damage	Large opening of the joints with probable damage due to impacts and considerable residual dislocation of the drums. No serious danger of collapse.
1.00	Near collapse	Very large opening of the joints, close to partial or total collapse.

5. Incremental dynamic analysis and fragility assessment results and discussions

Figure 5 reports IDA curves for the short column case (*a*) of the horizontal component (H) and horizontal and vertical component (H+V). The EDP threshold is represented in figure 5 as vertical dashed lines. The comparison between the IDA curves evidences a small influence of the vertical component of the ground motions on the overall trend. This is confirmed by the analytical and discrete fragility curves in figures 6a, 6b and form the comparisons in figure 6c, where it can be observed that the probability of exceeding the different limit states is quite similar in correspondence to the different PGA levels. In figure 7, IDA curves for the high column case (*b*) are reported for both H and H+V combinations of earthquake excitation. In this case, a significant reduction of the capacity is associated with the H+V combination. This can be also clearly observed from fragility curves in figure 8a and 8b and their comparison in figure 8c, where the H+V fragility curves appear clearly shifted on the left, except for the early damage limit state which seems being not significantly affected by the vertical component. A sample of the different damage configurations achieved by a column model (case *b*) during a time history analysis is also shown in figure 9, where the limit state thresholds achievement is highlighted.
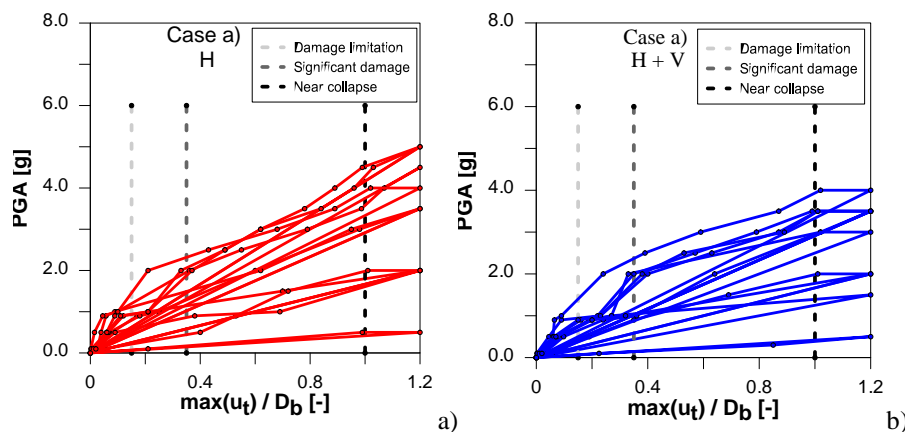

Figure 5. Case *a* IDA curves: a) horizontal component (H); b) horizontal and vertical components (H+V)
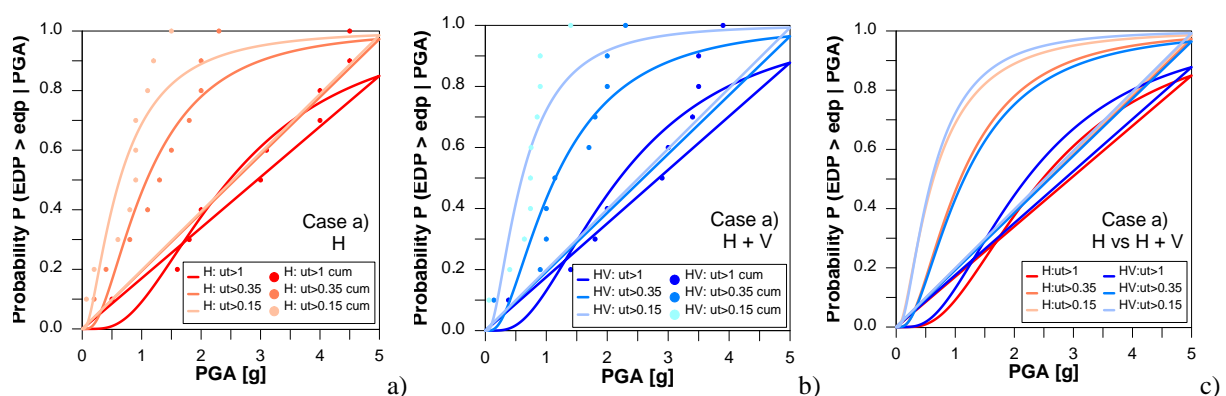

Figure 6. Case *a* analytical and discrete fragility curves: a) horizontal component; b) horizontal and vertical components; c) comparison between H and H+V combinations
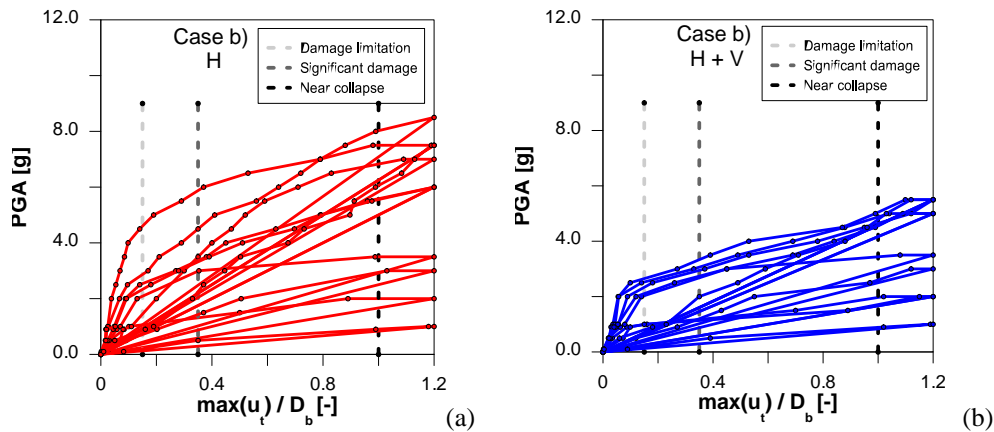
Figure 7. Case *b* IDA curves: a) horizontal component (H); b) horizontal and vertical components (H+V)
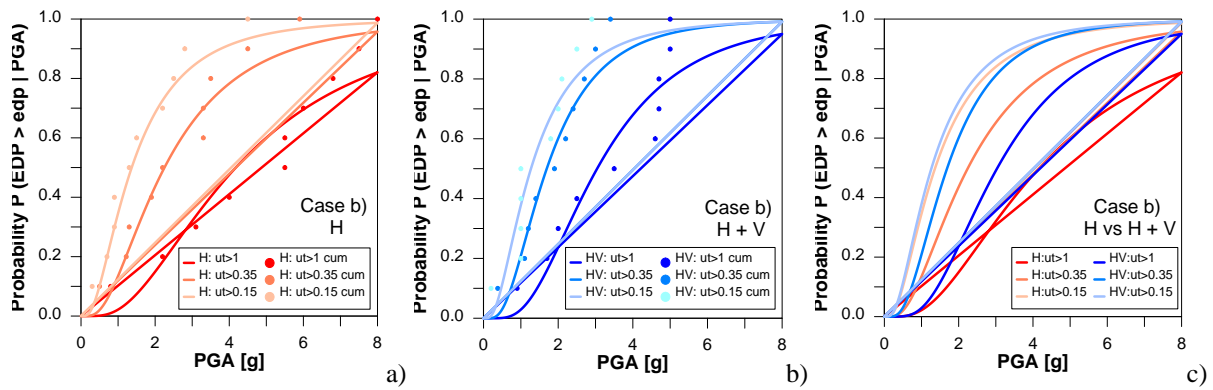

Figure 8. Case *b* analytical and discrete fragility curves: a) horizontal component; b) horizontal and vertical components; c) comparison between H and H+V combinations
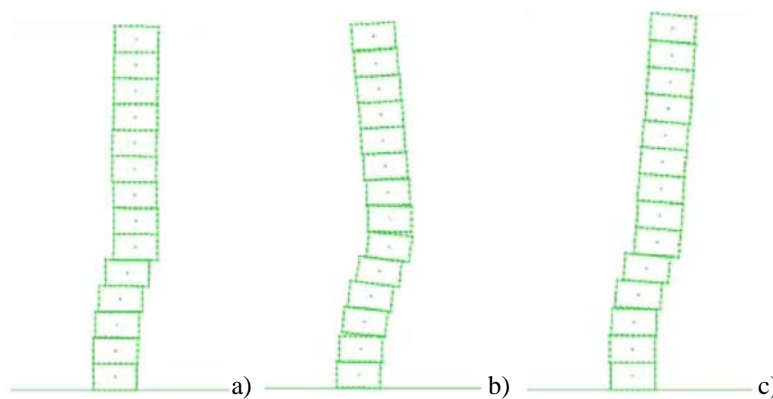

Figure 9. Case *b* model response to different u_t levels: a) damage limitation; b) severe damage; c) near collapse

The influence of the vertical component to the overall probability of collapse can be effectively measured by defining the parameter β as:

$$\beta = \frac{PGA_{c,50\%,H}}{PGA_{c,50\%,H+V}} \tag{5}$$

where $PGA_{c,50\%,H}$ is the PGA with the 50% probability of collapse, in case of the sole horizontal earthquake component and $PGA_{c,50\%,H+V}$ is the one with the 50% probability of collapse, in case of both horizontal and vertical components. For the case *a,* one obtains $\beta = 1.18$, therefore, estimations made by considering the sole horizontal component of the ground motion lead to a slight overestimation of the capacity in comparison with the case of considering both components. On the contrary, for the case *b* $\beta = 1.96$ is obtained. This brings the overestimation error to +50%.

Another consideration should be referred to the different fragility associated with the different column types, especially for the collapse limit state. The overall slenderness ratio of the two columns (H/D_b) is almost the same, while the slenderness of the respective drums (H_b/D_b) is quite different. Case *a* column drums are four times slenderer (H_b/D_b=2.14) than Case *b* column drums (H_b/D_b=0.6). The larger fragility associated with Case *a* column is clearly related to the slenderness of its drums which forces overturning collapse mechanisms rather than sliding. On the contrary, the Case *b* column has larger than high drums which strongly limit rocking while sliding is prevailing. The collapse is still associated with the overturning of the column, but this is induced by an excess of sliding. A comparison between Case *a* and Case *b* analytical fragility curves is shown in Figure 10.
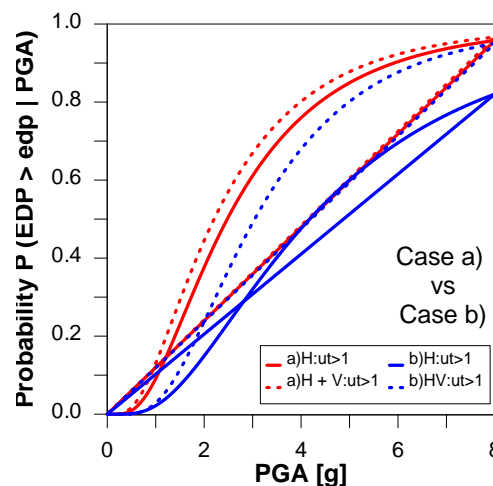

Figure 10. Comparison between Case *a* and Case *b* columns collapse limit state fragilities

6. Conclusions

The paper has presented the results of incremental dynamic analysis applied to two different typologies of classical columns with and without considering the simultaneous effect of the vertical component of the ground motions. IDA allowed determining fragility curves of the column in both the conditions and for three different limit states. Results obtained show that the slenderness of the drums is a key parameter influencing the overall collapse mechanism and therefore the fragility of columns. Column *a*, having three times the slenderness of column *b*, achieved collapse to PGA values reduced by 40%. A further conclusion can be drawn observing the effect of the vertical component of the ground motion on the fragility. Case *a* column has shown a slight influence of the vertical earthquake component on its overall fragility, on the other hand, noticeable reduction of the resisting capacity was found for the Case *b* column. Again, this can be related to the slenderness ratio of the drums, in fact, the rocking mechanism associated with the slender drums is less sensitive to the variation of vertical inertial forced. On the contrary, sliding mechanisms occurring between squat drums significantly depend on friction forces which are strongly altered during the variation of vertical inertial action.

References

[1]   G. Croci, The conservation and structural restoration of architectural heritage. *Advances in Architecture Computational Mechanics Publications*: *WIT Press*; 1998.

[2]   G. Croci, The collapse occurred in the Basilica of St. Francis of Assisi and in the Cathedral of Noto. *CIMNE: Structural analysis of historical constructions*; pp. 297–317, 1998.

[3]   P. Komodromos, L. Papaloizou and P. Polycarpou, Simulation of the response of ancient columns under harmonic and earthquake excitations. *Eng Struct;* vol. 30(8), pp 2154–64, 2008.

[4]   G. Augusti and A. Sinopoli, Modelling the dynamics of large block structures. *Meccanica*; vol. 27, pp. 195–211, 1992.

[5]   I. N. Psycharis and P.C. Jennings, Rocking of slender rigid bodies allowed to uplift. *Earthquake engineering & structural dynamics*; vol. 11, pp. 57–76, 1983.

[6]   C. S. Yim, A.K. Chopra and J. Penzien, Rocking response of rigid blocks to earthquakes. *Earthquake engineering & structural dynamics*; vol. 8, pp. 565–87, 1980.

[7]   P. A. Cundall, A computer model for simulating progressive large scale movements in blocky rock systems. *Proceedings of the symposium of the international society of rock mechanics*; 1971.

[8]   P. A. Cundall and R.D. Hart, Numerical modelling of discontinua. *Eng Comp*; vol. 9(2), pp. 101–13, 1992.

[9]   Itasca. UDEC - universal distinct element code manual: theory and background. *Minneapolis, USA: Itasca Consulting Group*; 2004.

[10] I. N. Psycharis, D. Y. Papastamatiou and A.P. Alexandris, Parametric investigation of the stability of classical columns under harmonic and earthquake excitations. *Earthquake engineering & structural dynamics*; vol. 1(29), pp. 1093–109, 2000.

[11] I.N. Psycharis, M. Fragiadakis and I. Stefanou, Seismic reliability assessment of classical columns subjected to near-fault ground motions. *Earthquake engineering & structural dynamics*; vol. 42(14), pp. 2061–79, 2013.

[12] B. Pulatsu, V. Sarhosis, E. M. Bretas, N. Nikitas, and P.B. Lourenço, Non-linear static behaviour of ancient free-standing stone columns. *Proceedings of the Institution of Civil Engineers - Structures and Buildings;* vol. 170 (6), pp. 406-418, 2017.

[13] V. Sarhosis, D. Baraldi, JV. Lemos and G. Milani, Dynamic behaviour of ancient freestanding multi-drum and monolithic columns subjected to horizontal and vertical excitations. Soil Dynamics and Earthquake Engineering 120, pp. 39-57, 2019.

[14] V. Sarhosis, J.V. Lemos, Detailed micro-modelling of masonry using the discrete element method. Computers and Structures, 206, pp. 66-81, 2018.

[15] V. Sarhosis, P. G. Asteris, A. Mohebkhah, J. Xiao and T. Wang, Three dimensional modelling of ancient colonnade structural systems subjected to harmonic and seismic loading. Structural Engineering and Mechanics. 40(4), Techno-Press, 2016.

[16] V. Sarhosis, P. Asteris, T. Wang, W. Hu, Y. Han, On the stability of ancient colonnades under static and dynamic conditions, Bulletin of Earthquake Engineering, pp. 1-22, DOI 10.1007/s10518-016-9881-z, 2016.

[17] C. A. Cornell and H. Krawinkler, Progress and challenges in seismic performance assessment. *University of California, Berkeley*: *PEER Center News;* vol 3, 2000.

[18] I. N. Psycharis, Seismic vulnerability of classical monuments. *European Conference on Earthquake Engineering;* pp. 563-582, 2018.

[19] F. Di Trapani, V. Bolis, F. Basone and M. Preti, Seismic reliability and loss assessment of RC frame structures with traditional and innovative masonry infills. *Eng. Struct;* 208; pp.110-306, 2020.

[20] F. Di Trapani, L. Giordano, G. Mancini, Progressive Collapse Response of Reinforced Concrete Frame Structures with Masonry Infills. *J. Eng. Mech.*; 146, 04020002, 2020.

[21] F. Di Trapani, M. Malavisi, Seismic fragility assessment of infilled frames subject to

mainshock/aftershock sequences using a double incremental dynamic analysis approach. *Bull. Earthquake Eng.*; 17(1), pp. 211–235, 2019.

[22] M. M. Maniyar, R. K. Khare and R. P. Dhakal, Probabilistic seismic performance evaluation of non-seismic RC frame buildings. *Structural Engineering and Mechanics;* vol. 33, pp. 725–745, 2009.

[23] F. L. A. Ribeiro, A. R. Barbosa and L.C. Neves, Application of reliability-based robustness assessment of steel moment resisting frame structures under post-mainshock cascading events. *Journal of Structural Engineering*; vol 140(8), pp. A4014008-1-12 2014.

[24] F. Basone, L. Cavaleri, F. Di Trapani and G. Muscolino, Incremental dynamic based fragility assessment of reinforced concrete structures: Stationary vs. non-stationary artificial ground motions. *Soil Dynamics and Earthquake Engineering;* vol. 103, pp. 105–117, 2017.

[25] F. Di Trapani, G. Bertagnoli, M. F. Ferrotto, and D. Gino, Empirical equations for the direct definition of stress–strain laws for fiber-section-based macromodeling of infilled frames. *Journal of Engineering Mechanics*, vol. 144(11), 04018101-1-17, 2018.J.W. Baker, Efficient analytical fragility function fitting using dynamic structural analysis. *Earthquake Spectra*; vol. 31(1), pp. 579–599, 2015.